Has been published in: Cellulose (2018) 25: 87-104

https://link.springer.com/article/10.1007%2Fs10570-017-1570-9

Changes in the hygroscopic behavior of cellulose due to variations in relative humidity

Lovikka, Ville A.;[*,§] Rautkari, Lauri;* Maloney, Thaddeus C.**

* Aalto University, School of Chemical Technology, Department of Forest Products Technology, P.O. Box 16300, FI-00076 Aalto, Finland

§ Department of Chemistry, A.I. Virtasen Aukio 1, P.O. Box 55, FI-00014 University of Helsinki, Finland

Corresponding Author

* ville.lovikka@helsinki.fi, +358-50-4989984; Orcid: *0000-0001-5412-9481*

KEYWORDS cellulose, water adsorption, solvent exchange, hornification, surface restructuring, critical point drying

Abstract

Details on how cellulosic surfaces change under changing moisture are incomplete and even existing results are occasionally neglected. Unlike sometimes reported, water adsorption is unsuitable for surface area measurements. However, water can be utilized for assessing surface dynamics. Hygroscopic changes of pulp and bacterial cellulose were studied by dehydrating the samples in a low polarity solvent and then introducing them into a moist atmosphere in a Dynamic Vapor Sorption (DVS) apparatus at 0-93 % Relative Humidity (RH). The DVS treatment caused hygroscopicity loss near applied RH maxima, however, the hygroscopicity increased at RH values > 10-20 % units lower. Additionally, the hygroscopic changes were partially reversible near the RH maximum. Therefore the hygroscopicity of cellulose could be controlled by tailoring the exposure history of the sample. Hornification reduced these changes. The observations support reported molecular simulations where cellulose was shown to restructure its surface depending on the polarity of its environment.

Introduction

An understanding of the behavior of cellulose under conditions of changing humidity is important for its applications as the hydration of cellulose, for example, reduces its adhesion and dimensional stability in composites (Hubbe et al. 2008; Siró and Plackett 2010). Although

cellulosic composites often need to resist physical changes over repeated exposure events at high and low humidities, research on cellulose behavior under repeated cycling has focused on the effect of water at or near its saturation point. In order to understand more fully the intricacies of the biopolymer, more detailed studies that focus on its behavior at subsaturation humidities are needed. One such topic is the drying of cellulose, which is a complex process that leads to an irreversible reduction in swelling and surface availability, known as hornification (Minor 1994). This, hornification, in turn reduces the reactivity of pulp (Khanjani et al. 2017; Nelson and Oliver 1971; Grethlein 1985) especially with repeated drying cycles (Leuk et al. 2015) due to irreversible microfibril aggregation or 'stiffening of the lignocellulose matrix' (Hult et al. 2001; Newman 2004; Suchy et al. 2010a and 2010b).

Cellulose behavior and its surface properties are defined by the prevalence of available hydroxyl groups (Dufresne 2012). Cellulose molecules consist of glucopyranose rings that have their hydroxyl groups oriented in equatorial positions whilst nonpolar C-H bonds are aligned in axial directions (Fernandes et al. 2011; Yamane et al. 2006). Moreover, cellulose molecules are partially ordered in crystalline structures that possess both hydrophobic and hydrophilic surfaces (Dufresne 2012; Medronho et al. 2015; Sinko et al. 2015). At the sub-micron level, cellulose is further organized into fibrillar structures that have a more disordered surface (Fernandes et al. 2011; Maurer et al. 2013) which have more potential for outward-directed hydroxyl groups when compared to perfect crystals. Research performed with liquids has shown that a non-polar environment causes a reduction in the hydroxyl group accessibility via different effects, for example, the hydroxyl groups can adsorb impurities from the environment, reorient themselves away from the fibril surface or create cross-linkages and aggregations (Yamane et al. 2006;

Johansson et al. 2011). Correspondingly, exposure to polar liquids has been shown to increase hydrophilicity (Bledzki and Gassan 1999) for the time of exposure despite the impact of hornification. Nevertheless, it would be beneficial to be able to distinguish between the effects of hornification and hygroscopic changes and to ascertain how permanent such changes are. Furthermore, cellulosic samples behave very differently < 96 % relative humidity (RH) when compared to that observed at levels above 96 %. Differences in water adsorption between different samples has been shown to be very small below 96 % RH and occasionally not even consistent with results at 99.98 % RH (Stone and Scallan 1967). This limits the applicability of research results achieved at water saturation to very specific conditions.

Structurally, it is estimated that there is a thin layer of non-crystalline cellulose on the surfaces of fibrils (Atalla et al. 2008; Fernandes et al. 2011; Leppänen et al. 2009; Salmén and Bergström 2009; Weatherwax 1977) that could be prone to hornification and interfibrillar hydrogen bonding to either cellulose or hemicellulose (Leppänen et al. 2009; Mohan et al. 2012). Modeling studies on a molecular level have also suggested that intrafibrillar restructuring can take place within the first molecular layers (Heiner et al. 1998; Matthews et al. 2006; Maurer et al. 2013), however, the nature and extent of such restructuring depend on the amorphous fraction and crystal structure of the surface (Kulasinski et al. 2017; Liao et al. 2012; Yamane et al. 2006). Figure 1 shows the possible changes including surface irregularities and hydrogen bond changes (red lines) from inter-chain (bulk cellulose, Fig. 1a) into inter-sheet bonds both in vacuum (Fig. 1b) and water (Fig. 1c) (Maurer et al. 2013). There is more inter-sheet bonding against vacuum (b) than against water (c) because water is able to attract hydrogen bonds. These type of structural changes lead to changes in the available hydroxyl groups on the fibril surface and therefore alter

the overall hygroscopicity of the cellulose. Importantly, if there is any delay or hysteresis in the surface restructuring, the surface could also have different configurations depending on what kind of environment they have been exposed to before the actual experiments.

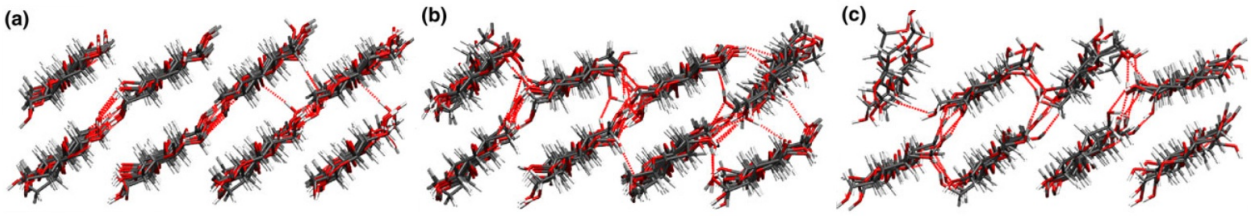

Fig. 1 Cross sections of cellulose Iα (100) in different environments. Some of the intra-sheet hydrogen bonds, which are typical to a) bulk cellulose, restructure into inter-sheet hydrogen bonds at the surface when the surface is exposed to b) vacuum or c) water. There are more hydroxyl groups pointing outward in water than in vacuum because water can attract hydrogen bonds. The figure is from Maurer *et al*. (2013) with permission from Springer

Critical point drying (CPD) with CO_2 can be used as a method to prepare dry cellulose with relatively intact pore structures in order to analyze the porosity, surface area and microscopic structure (Lovikka et al. 2016). While CPD is commonly employed together with N_2 sorption techniques, use in conjunction with water sorption studies is much more limited. In this study, we want to determine how the CPD procedure affects the water sorption characteristics of pulp fibers over a wide RH range, especially as the CPD method at least partially prevents hornification upon water removal. The CO_2 treatment may also cause surface molecule reorientation (Johansson et al. 2011) due to the low-polar nature of the treatment. Additionally,

the treatment has been previously shown to cause changes in the molecular distances on the cellobiose unit level when compared to interactions with water (Bazooyar et al. 2015).

The main aim of this study is to understand how cellulose surfaces behave as relative humidity (i.e. water activity) is changed below its saturation point by using CPD in combination with Dynamic Vapor Sorption (DVS). In this paper, we show that the subsaturation RH behavior of cellulose is more complex than is sometimes assumed as cellulose surfaces can both gain and lose hydrophilicity with only small changes in humidity. This can have a profound impact on the reliability of both cellulose analysis methods and applications. Differently predried samples were studied to understand to what extent the hygroscopicity of cellulosic surfaces can be changed by surface restructuring, how stable these changes are and whether hornification can be used to prevent such changes.

Materials and methods

Samples and solvents

Various bleached pulps were used for the study as shown in Table 1. “Never dried” samples (ND) were never dried prior to the solvent exchange and Critical Point Drying (CPD) protocol. Other samples were either dried in 100 °C (“oven dried”) overnight or were acquired as regular

123 industrial pulp sheets (“machine dried”). These samples with different drying histories (“predried
124 samples”) underwent cold redispersion to water before being subjected them to the same solvent
125 exchange and CPD protocol. The K-100-Ref in the Table 1 is similar to sample K-100 except
126 that it was not redispersed or CPD treated. Samples primarily comprised of fully bleached birch
127 (*Betula spp*.) pulp with the addition of a sample of bacterial cellulose (from *Gluconacetobacter*
128 *medellensis*). The bacterial cellulose (BC) preparation method has been described elsewhere
129 (Castro et al. 2012). Acetone (VWR International) was at least of 99.5 % purity, CO_2 (Oy Aga
130 AB) was of at least 99.8 % pure and deionized water was used throughout the experiments.

131

132 **Table 1**. The samples used in this study. All the pulp samples were bleached. N.B. the table is
133 partially taken from Lovikka *et al*. (2016) with permission from Elsevier

Name	Species	Type	Drying	Hemicellulose content (%)
d-ND	birch	dissolving	ND	6.6
d-d	birch	dissolving	machine dried	6.0
d-100	birch	dissolving	oven (100 °C)	6.1
K-ND	birch	kraft	ND	26.1
K-100	birch	kraft	oven (100 °C)	26.0
K-100-Ref	birch	kraft	oven (100 °C)	26.1
BC	*G. medellensis*	bacterial	ND	0

134
135

136

137 Solvent exchange and critical point drying

Pulp samples (with 10 % solid content) were placed into 50 kDa molecular weight cut-off (MWCO) regenerated cellulose membrane tubings and the pulp was solvent exchanged by dialysis with acetone for over 45 hours in the presence of a magnetic stirring. The acetone was subsequently exchanged with liquid CO_2 in a critical point drier (Leica EM CPD300) over 25 CO_2 partial exchange cycles which lasted 1 hour in total. Next the CO_2 was heated to 35°C under ~75 bar pressure in order to bring it into the supercritical state and this fluid was slowly vented out until only carbon dioxide gas at atmospheric pressure remained for the fluid phase. After CPD was complete, the samples were immediately transferred either to DVS or the N_2 sorption apparatus following the method described previously (Lovikka et al. 2016).

Dynamic Vapor Sorption (DVS)

H_2O sorption was measured with a Dynamic Vapor Sorption equipment (DVS Advantage ET, Surface Measurement Systems). The weight of the sample was monitored with a microbalance whilst a constant flow of nitrogen of predetermined water content was used to control the RH within the sample chamber. The sorption-desorption isotherm cycles were collected sequentially for the same sample and the sample Equilibrium Moisture Content (EMC) was recorded after the mass change rate stayed below 0.002 %/min continuously over a 10-minute period. The device was equipped with a calibrated RH sensor (Rotronic HC2-IC, Switzerland) that allowed the true RH in the chamber at each step to be recorded. These results showed that the measured value was 1-2 % units lower than the set value. The measured RH values are used in the later sections. The temperature within the sample chamber was kept constant at 24 °C (±0.05 °C) and the setup was additionally enclosed by an insulating box.

The measurement protocols comprised of either a 2-cycle or multicycle step process. For the 2-cycle measurements, the target humidity was increased both times in 5 % increments from zero to 95 % RH with two additional steps during the adsorption phase at 2.5 % and 7.5 % (see for an example isotherm Fig. 2a). The multicycle runs (d-ND-g and K-ND-g) were performed using a more complex program. Dissolving pulp (d-ND-g) was measured using a first cycle with a maximum at 20 % RH. Each subsequent cycle carried out was 10 % RH higher than the previous maximum until a cycle at RH 90 % was completed. After that the sample was exposed and dried from 95 % RH without intermediate steps before one more full cycle with intermediate steps to 90 % RH was completed. These cycle maximum values are presented in Table 2 in chronological order. Data was only collected at every 10 % RH increase with the exception of an additional measurement step at 5 % RH. For the kraft pulp sample (K-ND-g) cycles 60 % and 70 % RH were repeated after the first exposure to 70 % RH. The last cycle of K-ND-g was set to 95 % RH instead of 90 % used for d-ND-g.

Table 2. The progressively higher cycles in the DVS measurements. Cycles with * were completed without any intermediate steps (0% → 95% → 0% RH)

SAMPLE NAME	RH AT EACH CYCLE MAXIMUM (%)
d-ND-g	20, 30, 40, 50, 60, 70, 80, 90, 95*, 90
K-ND-g	20, 30, 40, 50, 60, 70, 60, 70, 80, 90, 95*, 95

178 The specific surface areas were determined with both N_2 and H_2O. Measurements with water
179 were analyzed with the Guggenheim-Anderson-de Boer method (GAB), which can be applied
180 over a more extended range when compared to the classical BET equation (Brunauer et al. 1938;
181 Timmermann 2003). GAB was chosen, since water sorption on cellulose is specific at low RH
182 and there is no well-defined cellulose surface when water is used as the probe molecule, which
183 means that the BET method is ineffective for such H_2O sorption studies (Greyson and Levi
184 1963). Nevertheless, both methods are still being used and therefore they need further
185 examination (Häggkvist et al. 1998; Ioelovich and Leykin 2011; Espino-Pérez et al. 2016).

186

187 Kinetic analysis of DVS

188 The kinetics of the Dynamic Vapor Sorption (DVS) was studied with one of two methods: i)
189 Parallel Exponential Kinetics (PEK) model or ii) simply comparing the lengths of each sorption
190 step. The PEK method assumes two parallel, independent first order processes and relies on the
191 following parallel exponential equation (Kohler et al. 2006):

192 $$M_t = M_{inf\,1}\left(1 - e^{-t/t_1}\right) + M_{inf\,2}\left(1 - e^{-t/t_2}\right) \quad (1)$$

193 where M_t is the sample mass at a given time t, M_{inf} mass at equilibrium, t_1 and t_2 the time
194 characteristic times for the two sorption processes. The sensitivity of data fitting was studied by
195 comparing the results, when the first data points were masked either by 30 seconds or until the
196 maximum slope of the curve was reached. The kinetics were also studied by a simple plotting of
197 the running times of each measured step against the target relative humidity. Average sorption

198 rates for each step were calculated by dividing the total mass change by the total time spent for
199 the step.

200

201 N_2 sorption

202 N_2 sorption was analyzed for samples before and after DVS to monitor porosity changes during
203 the DVS treatment. Specific surface areas (SSA) were measured at 77 K by nitrogen sorption
204 apparatus (Tristar II, Micromeritics) and the data was analyzed using a Tristar 3020 software
205 (Micromeritics). Approximately 150 data points were collected between the relative pressure of
206 0 and 0.99 for the isotherms and the surface area was determined using the Brunauer-Emmett-
207 Teller (BET) equation (Brunauer et al. 1938) at relative pressures between 0.05 and 0.35 where
208 the BET fitting was observed to be good. The method and the results of N_2 sorption have been
209 recently published in more detail (Lovikka et al. 2016).

210

211 Scanning Electron Microscopy (SEM)

212 Samples were prepared from fresh Critical Point Dried (CPD) samples although brief exposures
213 to humid air were possible. Single fibers were pulled from the samples with carbon tape and care
214 was taken to avoid any unnecessary fiber compression. Samples were then sputtered with a 3 to 9
215 nm layer of gold prior to imaging with the secondary electron detector of a Sigma VP (Zeiss)
216 with an acceleration voltage of 1.2-1.5 keV.

217

Results

DVS isotherms

Water adsorption behavior of the samples changed over repeated cycles of DVS measurements. The sorption cycles in two-cycle measurements were different from each other until the desorption phase between 20-40 % RH where the two cycles coincided (Fig. 2a, steps 2 and 4). Additionally, although the samples adsorbed less water during their second cycle at high RH as expected due to hornification, the adsorption was significantly increased at low and medium RH in comparison to the values from the first cycle (Fig. 2a, steps 1 and 3). To best of the authors' knowledge, this increase in the hygroscopic nature of cellulose under relatively mild conditions have not been reported previously. Remarkably, although the first cycle isotherms are often compared in the literature, the differences between the same sample isotherms (Fig. 2a) were sometimes larger than between the same cycle isotherms of different samples (Fig. 3a and 3b).

The same hygroscopic changes seen in d-ND were observed to proceed, although more gradually, in the corresponding multicycle run, d-ND-g. In Fig. 2b the d-ND-g isotherms are plotted against d-ND and it clearly shows how the d-ND-g curves largely follow the second cycle of d-ND. The measurement points of d-ND-g with the largest deviations from d-ND are the new RH highs, which are located between the first and second cycle adsorption curves of d-ND at RH > 50 % and slightly below them at RH < 40 %. When the next cycle of d-ND-g reached

239 the previous RH high, adsorption was always determined to be lower than the first time (Fig. 2c).
240 If the sample was exposed to and subsequently dried from a 10-20 % units higher RH, the
241 sorption started to increase again at that RH. At humidities < 40 % RH the highest EMC
242 (Equilibrium Moisture Content, %) was reached only after 3 or more adsorption cycles to higher
243 RH values. This was counter intuitive since cellulose is generally known lose its initially porous
244 structure (Fig. 2d) upon exposure to water and as a result the sample would have been expected
245 to adsorb the most water during the first cycle.

246

247

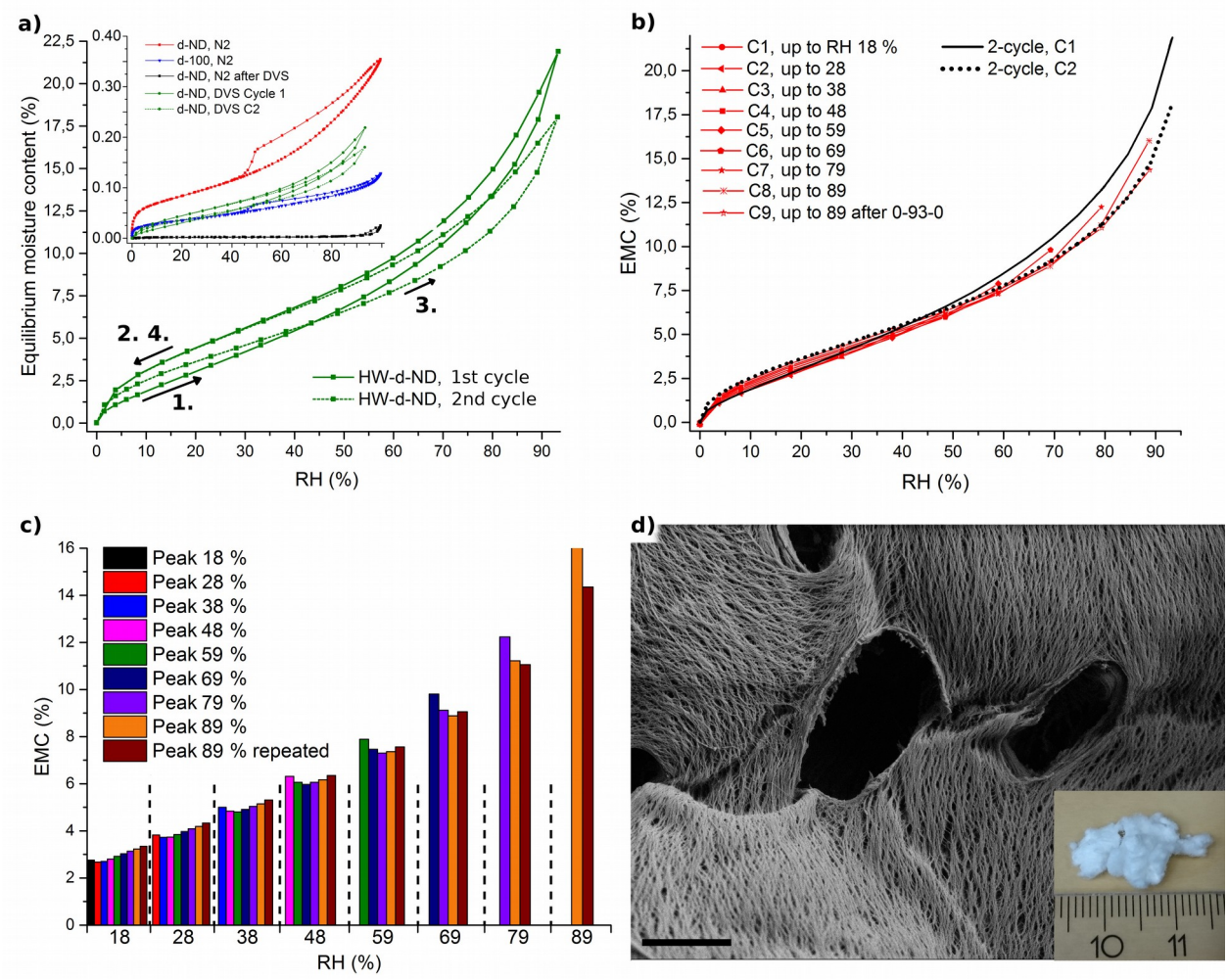

248 **Fig. 2** DVS isotherms. a) Whole isotherms of d-ND and comparisons (inset) to the corresponding
249 N_2 adsorption isotherms. The units for the x- and y-axis in the inset are % and ml/g, respectively.
250 b) Nine adsorption branches of d-ND-g (red lines, “C1-C9”) compared to the 2 cycles of d-ND
251 (black, “C1-C2”). c) EMC values of d-ND-g presented as columns. d) SEM image and a
252 photograph (inset) of a d-ND sample. Scale bar is 2 µm. N_2 isotherm details in a) are reprinted
253 with permission from Elsevier (Lovikka et al. 2016)

254

255 Reversibility of the changes during repeated cycling

A multicycle run, with K-ND-g, was performed in a similar fashion to that for the d-ND-g sample. The main difference was that for the K-ND-g the measurement cycles to 60 % and 70 % were repeated after the first adsorption cycle to 70 % RH (Fig. 3c). During this repetition, the adsorption of K-ND-g showed increasingly complex hygroscopic changes as the measurement approached the exposure maximum. At 18 % RH, the repeated cycles did not result in any notable change. At 28 and 38 % RH, the adsorption was increased after the first exposure cycle to 59 and 69 % RH, however, the second exposure to 59 % resulted in a slight reduction in adsorption whereas the second exposure to 69 % RH returned it to the level observed prior to the repetition cycles. In other words, the exposure to 59 % RH seemed to cause the adsorption to converge towards some value whereas 69 % RH only leads to increased adsorption. At 48 % RH, the sorption was lowered by both cycles to 59 % RH but increased with the cycles to 69 % RH. In contrast, at 59 % RH the sorption was smaller after both cycles to 59 % RH and the first to 69 % RH but was larger after the second exposure to 69 % RH, whereas the adsorption at 69 % RH was reduced even after the second cycle to 69 % RH. After the repetition cycles, an exposure to 79 % RH was needed to reach new EMC maxima below 69 % RH.

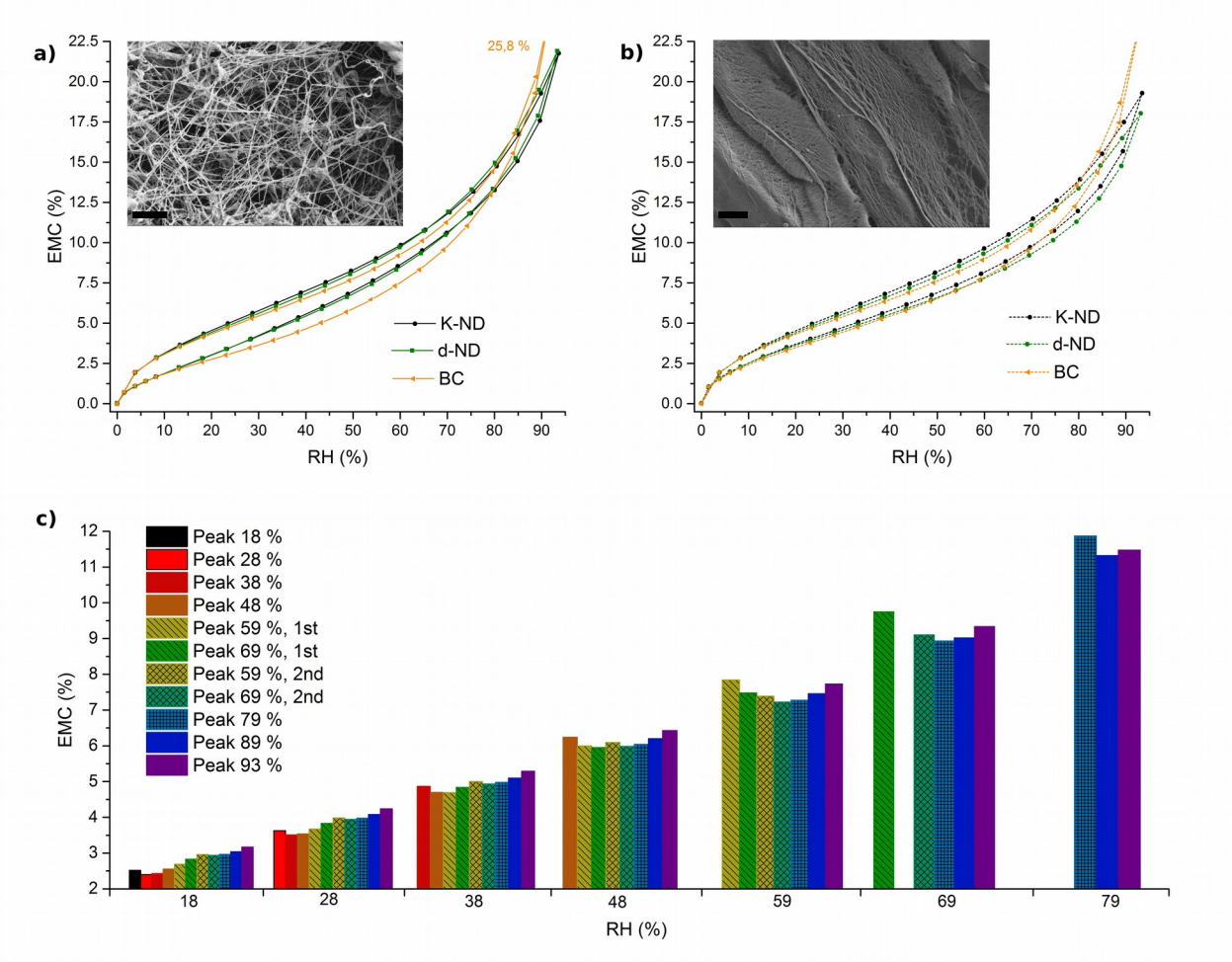

273 **Fig. 3** DVS isotherms. a) First cycles of the ND samples, SEM image of BC as an inset; b)
274 second cycles of the ND samples, SEM image of K-ND as an inset; c) K-ND-g isotherm data
275 presented as columns. Both scale bars represent 1 µm

276

277 Other cellulose sources: BC and kraft

278 In general, K-ND behaved much like dissolving pulp except that the changes to the hygroscopic
279 nature of K-ND were smaller. Both samples adsorbed similar amounts of water even though

dissolving pulp possesses less hemicellulose than kraft pulp (Fig. 3). During the first cycle, d-ND sorbed marginally less water than the K-ND between RH 28-79 % but had a slightly higher EMC after exposure to 79 % RH, during the second cycle, d-ND sorbed less than K-ND also at high RH.

Bacterial cellulose, which consists of cellulose only, showed two large differences in comparison to the pulp samples (Fig. 3). During the first cycle, BC behaved in a similar manner to pulp at RH 0-13 % but adsorbed water much less than pulp at 13-79 % and much more at 79-93 %. During the second cycle the differences between pulp and BC below 69 % RH were significantly smaller. Another BC sample was compressed into a film during the drying procedure, making the interfibrillar distances smaller than in the non-compressed BC sample. The compressed sample sorbed up to 12 % more water than the BC aerogel after 33 % RH but otherwise the isotherm looked very similar to that of the uncompressed sample isotherm (results omitted for clarity).

The effect of predrying on the hygroscopic changes

The 2-cycle protocol was applied to the dissolving and kraft pulp samples with different drying histories. The measured maximum sorption of the ND samples was found to be higher than those of the predried samples as expected. The ND samples also showed the largest deviation between the two cycles. The predried samples had first cycle adsorption curves that were intermediate versions of the first and second cycles of the ND samples (Fig. 4). During the first desorption, the K-100 sample approached K-ND isotherm until they intersected at 18-38 % RH, whilst the

second cycles of K-100 and K-ND were comparative. The same behavior was also observed for dissolving pulp once the sample weight loss during the first desorption cycle of d-100, possibly due to trapped solvent, was taken into account.

Predrying had a surprising effect at low RH values as samples d-100 and K-100 sorbed more water than their ND counterparts during the first adsorption phase. K-100 adsorbed 11 % more water than K-ND and d-100 adsorbed 7 % more than d-ND during the first cycle at 18 % RH. D-ND and K-ND started adsorbing more than the oven-dried samples only after RH 43 % and 59 % RH, respectively. Nevertheless, the differences with dissolving pulp may be underestimated because trapped solvent caused both d-d and d-100 to lose 0.27 % and 0.20 % of their weight during the first cycle, respectively. This difference was almost as large as the difference between d-ND and predried dissolving pulp samples during the first cycle desorption below 50 % RH. The d-100 sample behaved like d-d except that it adsorbed marginally more around 8 % RH and slightly less at > 38 % RH. Similarly, K-100 was found to adsorb more water than K-100-Ref except for the RH range between 0-18 %. During the second cycle the differences between ND samples and their oven-dried counterparts were smaller. For dissolving pulp, when the sample weight losses during the first cycle have been compensated, the difference is 2.2 and 2.3 % at 18 % RH during adsorption and desorption but increases starting from 2.6 % at 54 % RH to up to 8.9 % by 93 % RH. For kraft pulp the difference between ND and 100 was 1.1 % and 1.3 % during adsorption and desorption at RH 18 %, respectively, but the difference increased starting from 1.6 % at 69 % RH to up to 6.2 % by 93 % RH.

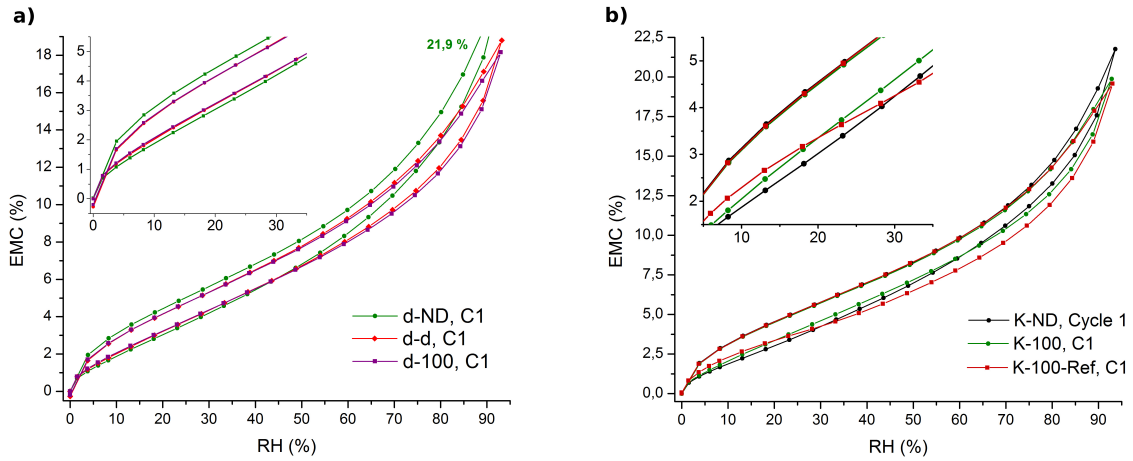

Fig. 4 The first cycle isotherms for the 2-cycle samples. a) Effect of predrying on dissolving pulp, detail of low RH range as inset, b) effect of predrying on kraft pulps, detail of low RH range as inset

DVS hysteresis

Hysteresis, defined here as the difference between adsorption and desorption divided by adsorption highlights the observed behavior of the different celluloses investigated at low and high RH (Fig. 5). Typical literature values for pulp hysteresis normally show upward slopes for pulp (Hill et al. 2009), natural fibers (Xie et al. 2010) and wood (Jalaludin 2011; Kymäläinen et al. 2014; Willems 2014a and 2014b) samples. The samples used in this study also had similar curve profiles in the second measurement cycle, though the first cycle hysteresis curves had a tendency to deviate from the literature curves in two ways. At low RH levels, the curves showed a secondary peak at circa 18 % RH, which is obviously due to lowered adsorption during the first DVS cycle, whereas at high RHs the samples had smaller hysteresis than the second cycle

curves. The hysteresis values at 18 % RH were plotted against the reported N_2 SSA values for the samples (Fig. 5b). For the pulp samples, there was an obvious correlation between the two values during the first cycle. In contrast, during the second cycle, the samples were more hornified and the hysteresis remained close to 0.79 for all the samples, indicating that more than half of the hysteresis anomaly at RH 18 % is independent of sample porosity. BC showed the largest changes in hysteresis at 38-48 % RH whereas pulp remained relatively unchanged across that range.

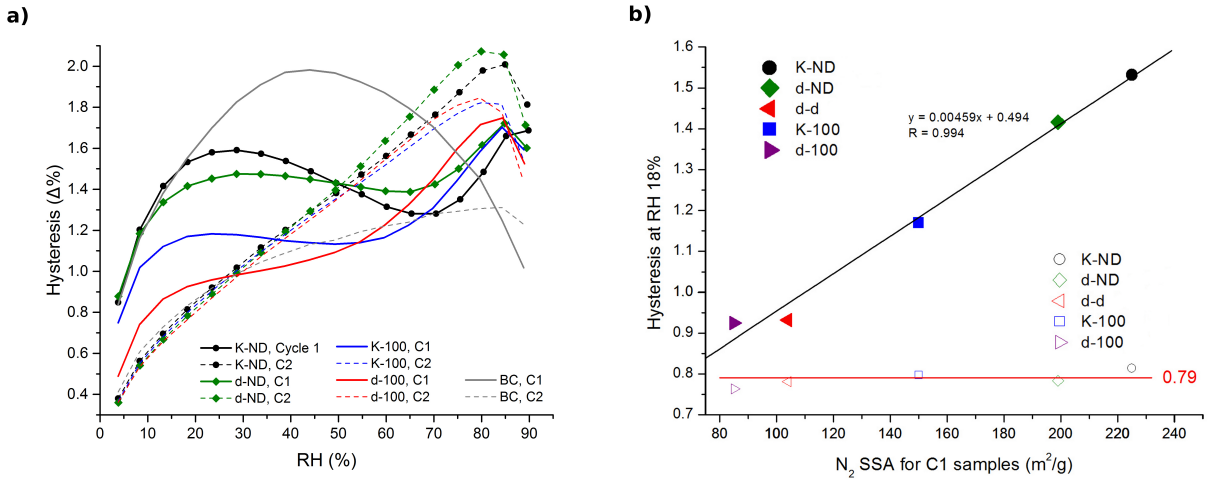

Fig. 5 a) Hysteresis curves of some DVS samples. b) The hysteresis values at 18 % RH plotted against N_2 SSAs measured before the first DVS exposure. The full symbols are for the first (C1) and the empty symbols for the second DVS cycle (C2) values. The N_2 values are reprinted with permission from Elsevier (Lovikka et al. 2016)

352 Water sorption kinetics

353 In general, adsorption was faster than desorption (Fig. 6a) which can be seen both in the shorter
354 step lengths and quicker sorption rates. This was especially pronounced during the first cycle at
355 RH values > 23 % where the difference between adsorption and desorption (Fig. 6a, the first
356 inset) increased during the first cycle but subsequently reduced during the second. When
357 adsorption and desorption rates were plotted, all the curves (except for the first sorption curve)
358 showed a U-shaped behavior common for natural cellulosic fibers (Xie et al. 2010) (Fig. 6a, the
359 second inset). With the exception of the first adsorption, the sorption rates decreased until 38 %
360 RH when reading the graph from the origin. The adsorption and desorption rates increased again
361 at > 69 % RH, which corresponds to EMC contents of > 10 %. However, it should be noted that
362 in this work the kinetics data points < 8 % RH and > 89 % may not be fully comparable due to
363 their shorter step lengths that might affect the results as previously shown for wood (Christensen
364 1959).

365

366 Kinetics were also analyzed using the PEK model but the method was unable to provide
367 satisfactory results even with high R^2 values (> 0.999). If the first data points were not masked,
368 the fitting residuals fluctuated strongly during curve fitting as observed previously by Driemeier
369 *et al*. (2012). This fluctuation has been attributed to variations in the data, possibly because of
370 small changes in temperature due to feedback system (Hill et al. 2012). In our measurements
371 reservoir temperature changes were typically in the range of ± 0.02 °C during a single exposure
372 step. Nevertheless, the residual fluctuations were possibly magnified by the slow onset of the
373 water adsorption as the residuals became smaller when more data points were masked before

curve fitting. Nonetheless, utilization of this method caused the coefficients t_1 and t_2 (equation 1) to increase and especially t_2 started to fluctuate across the measured RH range occasionally to an unacceptable extent. Therefore the results were considered to be too sensitive to the data pretreatment and the analysis was discontinued.

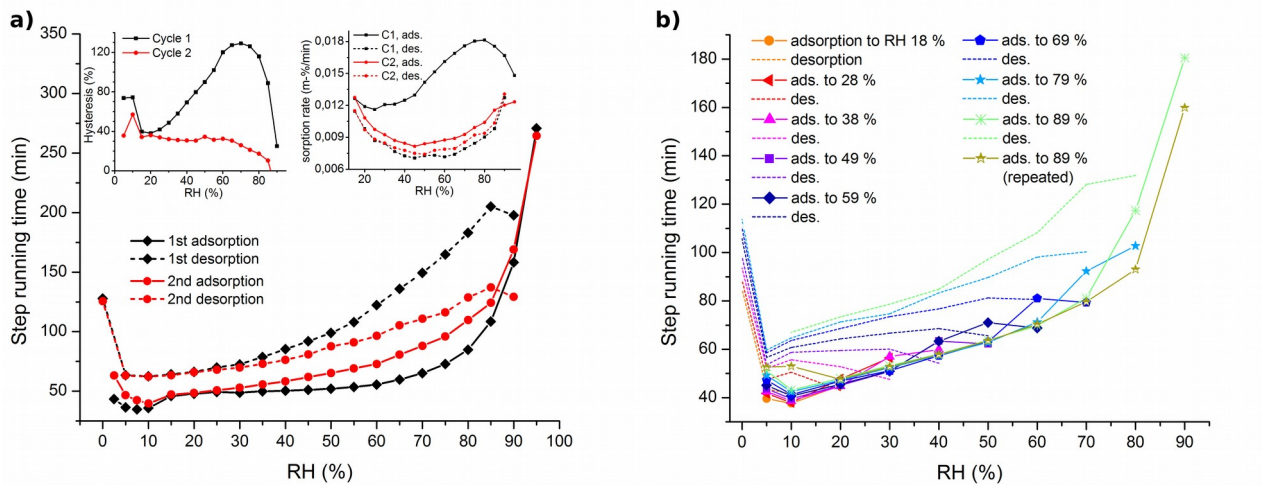

Fig. 6 Measurement running times and the rates of sorption. a) Data for d-ND. Hysteresis for both of the cycles are presented in the left side inset. The average rates of sorption are shown for each step in the right side inset. b) Data for d-ND-g

Comparison of H_2O and N_2 adsorption data

Specific surface area (SSA) determined by DVS was found to be relatively insensitive to the sample differences, meaning these measurements proved to be inconclusive with both BET and GAB methods. For example, BET and GAB analyses of DVS data gave similar SSA values

(108-149 m^2/g and 135-188 m^2/g, respectively) for the samples in spite of fibril aggregations, hornification and SSA differences over two orders of magnitude observed in N_2 adsorption (2nd and 4th column in Table 3).

Table 3. Specific surface areas by nitrogen and water adsorption. Values with * are averages from multiple measurements with standard deviation of 5-13 % (± 2σ) and are reprinted with permission from Elsevier (Lovikka et al. 2016)

SAMPLE NAME	N_2 SSA (m^2/g)	H_2O SSA; Cycle 1 / Cycle 2 (m^2/g)	N_2 SSA after DVS (m^2/g)
d-ND	199*	135 / 130	4.8
d-d	104*	136 / 125	4.5
d-100	85*	134 / 125	3.5
K-ND	225*	135 / ca 144	5.5
K-100	150*	149 / 136	1.7
K-100-Ref	-	122 / 137	-
BC	253	108 / 126	66.7

It is worth noting that in some of our samples H_2O adsorption was lower than N_2 adsorption, according both to SSA values and total volume adsorbed. For pore volume comparisons, both N_2 and H_2O isotherms were adjusted to the same units (liquid volume / sample weight) and plotted on the same graph (Fig. 2a inset). As can be seen, especially at low relative humidities, nitrogen is sorbed to a more significant degree, although this comparison is probably complicated as a result of diminishing sample volume due to the cryo conditions used during N_2 sorption. At room temperature the samples were found to be highly porous (Fig. 2d) before exposure to water (Lovikka et al. 2016).

Discussion

The hygroscopic properties of the surface were affected by water during both adsorption and desorption phases. This can be seen in the 2-cycle data where the two cycles differ from each other until they have similar desorption branches at low RH region. Similar observations have been reported for isotope labeled cellulose (Sepall and Mason 1961) and wood after thermo-modification at 220°C (Chirkova et al. 2009). With DVS the end point of changes could be located quite precisely, for example, the changes were completed for d-ND by 18 % RH during desorption of the first exposure cycle (Fig. 2a). The nature of these hygroscopic changes is later discussed more in detail based on observations on isotherm shapes, hysteresis and simple adsorption kinetics.

When samples were initially placed in the 0 % RH atmosphere, small weight losses of -3 % and -4.5 % were typically detected for pulp and BC, respectively. The presence of this additional weight could have been re-adsorbed moisture during the sample transfer. Other researchers have used more extensive protective measures (Weatherwax and Caulfield 1971) to prevent moisture re-adsorption and structural collapse. Nonetheless, the very high SSA values for kraft pulp before DVS analysis, up to 225 m^2/g for birch (Lovikka et al. 2016), showed that the method used here was adequate and therefore the samples were also assumed to have preserved their surfaces in freshly dried state. Although some effect on the sample properties especially at low RH cannot be ruled out, the effect should be similar to those reported in this paper. Therefore the

effect due to the re-adsorption would be only to reduce our DVS observations in scale by pre-emptive hygroscopic changes, however, all the samples showed further changes even at the lowest measured RH's, once they were exposed to high enough RH's. In continuation to this, it is hypothesized that similar surface structure changes could continue both at low and high RH values at water activities beyond ambient room conditions, e.g. with supercritical water or water in nanoconfinement. Studying the latter could have beneficial effects on biocomposite development.

The sample equilibration times were not long enough to observe the samples in full equilibrium with vapor because cellulosic samples might not equilibrate even during 2-day long exposure steps (Glass et al. 2017). Because the full measurements would take months or years to complete, more commonly used step length protocol was applied (< 0.002 %/min over 10 min). Even the shorter steps are long enough to observe major changes in the EMC's (Glass et al. 2017; Hill et al. 2009). Additionally, because the observed differences between the samples and the cycles are large and systematic in the consistent experimental conditions, it is unlikely that the qualitative results would change even with longer step lengths. However, the reader is encouraged to keep in mind that quantitative results are dependent on the applied equilibration times.

Nature of the hygroscopic changes

The anomalously low sorption determined during the first exposure cycle may be due to surface restructuring and changes in the hydroxyl group accessibility caused by the nonpolar solvent

sample treatments (Johansson et al. 2011; Maurer et al. 2013, Yamane et al. 2006). This was possibly enhanced by the presence of supercritical carbon dioxide which is able to penetrate cellulose (Zheng et al. 1998). Importantly, the hygroscopic changes during adsorption were not limited to any specific RH range even though different phenomena dominate water adsorption at different RH's. Interestingly, the hygroscopicity could both increase and decrease even at low RH values where sorbent-sorbate interactions define the adsorption (Kulasinski et al. 2017; Sing et al. 1985), whereas hornification should only reduce the adsorption by increasing hydrophobicity through macromolecular ordering (Mohan et al. 2012) and reducing porosity (Fernandes Diniz et al. 2004). Adsorption in mesopores or swelling are unlikely as they are typical only when Equilibrium Moisture Content (EMC) is > 5 % or > 15 % RH (Grunin et al. 2015; Hill et al. 2009; Kulasinski et al. 2015, 2017; Salmén 1982). Water adsorption data remained almost unchanged even when N_2 SSA showed significant porosity loss caused by the DVS analysis, which indicates that mesoporosity changes should not affect DVS values very strongly. Although cellulose itself can exhibit strongly increasing adsorption at high humidities (Banik and Brückle, 2010; Hill et al. 2009), the upward bend at the high RH end of adsorption isotherms has previously been also attributed to the presence of hemicelluloses (Engelund et al. 2013; Köhnke and Gatenholm 2007; Oksanen et al. 1997). In the measurements outlined here, however, BC that does not contain hemicellulose nor any similar interfibrillar capillary structure due to its random fibril arrangement also showed increased amounts of water sorption at high RH. The results suggest that these changes in the samples must be at least partially independent from their capillary structures or exact chemical compositions. In comparison, the adsorption isotherm of BC changed more than that of pulp samples over repeated cycling, possibly as a result of the Iα structure of BC, which is more labile than the Iβ cellulose in higher plants

(Dufresne 2012). Additionally, as the measurements were carried inside a closed chamber, contaminations were unlikely, therefore, the mechanism behind the hygroscopicity changes was likely due to surface restructuring in these samples.

Interestingly, the hygroscopic changes were smaller for samples with prior drying history. Since predried samples are more crosslinked and aggregated than never dried samples due to hornification, rearrangements of their surfaces into other configurations may have been restricted (Lang and Mason 1960). In other words, the hornification may have prevented surface restructuring during our low-polarity treatment and this would have helped to keep the hydrophilic moieties facing the fibril surfaces until the DVS measurements. The preventive effect against hygroscopic loss at low RH's was observed to be stronger in samples with a more severe predrying history, possibly because the hornification was less reversible in them as shown previously by Stone and Scallan (1966). Once the samples were exposed to high humidities in the DVS device, the presence of high water levels may have increased the hygroscopicity by triggering hydroxyl group reordering back towards the surface. After the first exposure cycle the never dried samples hornified as well, which can be seen in the similarities of cycle 2 isotherms between d-ND and the predried samples (Fig. 4a and its inset). Overall, a change in the hygroscopic nature and hypothesized hydroxyl group reorientations mean that the hydrogen bond pattern of cellulose would change as the samples are exposed to different humidity cycles. This might be related to the unexpectedly complex hornification and its reversibility reported recently for wood (Thybring et al. 2017). An interesting additional consequence of the hydroscopic changes of cellulose is that if hydrogen nuclei could be exchanged directly between cellulose hydroxyls without intermediate water, the change in the hydrogen bond network could create

proton transfer chains between the surface and subsurface parts of cellulose. This could be problematic for cellulose analytics, like deuterium labeling, although the authors are not aware of reported issues which could be unambiguously shown to be caused by this purely speculative phenomenon.

In general, hysteresis has been linked to various factors and therefore its interpretation is not straightforward. Hysteresis at low RH has been related to non-complete wetting at the nanoscale due to impurities (Cohan 1938), but as the sorption cycles were performed in a sealed DVS sample chamber, impurities do not explain the changes in hysteresis in different cycles. Moreover, according to Cohan, impurities should also lead to non-closed N_2 sorption curves, which was not observed previously (Lovikka et al. 2016). Also, hysteresis in the isotherms has previously been linked to the presence of hemicellulose (Engelund et al. 2013) and indeed kraft samples gave slightly more pronounced hysteresis curves than the dissolving pulps. Nevertheless, the presence of hemicellulose is unable to explain why hemicellulose-free BC gave rise to a stronger hysteresis than that observed for pulp. High sorption at low RH values has been linked to lower sample crystallinity (Mihranyan et al. 2004) and this would suggest that the samples measured here would have lost crystallinity during the first water exposure cycle but this is contradicted by the results in the literature. The highest level of hysteresis at low RH was observed with a sample of relatively low crystallinity (Xie et al. 2011) and crystallinity has also been reported to be increased with a drying-rewetting cycle (Newman 2004), however, sample crystallinities were not analyzed as part of this study.

Additionally, hysteresis has also been linked to slow, glassy relaxation in the material (Engelund et al. 2013; Willems 2014b) as moisture induces glass transition within amorphous cellulose at room temperature when EMC > 10 % (Salmén 1982). This softening allows more sorption, which would cause an upward bend in the isotherms and the kinetic data at 70 % RH, both of which agree qualitatively with our data. This limit, at approximately 70 % RH or 10 % EMC, is also where water diffusion has been shown to increase strongly (Kulasinski et al. 2014; Topgaard and Söderman 2001; Zografi and Kontny 1986). Prior to this RH, specific sorption and water clustering around polar or charged groups (Bazooyar et al. 2015; Belbekhouche et al. 2011; Berthold et al. 1996; Cohan 1938; Kulasinski et al. 2017; Maurer et al. 2013; Newns 1973; Olsson and Salmén 2004) or a more tortuous diffusion path between the fibrils (Topgaard and Söderman, 2001) might slow down water mobility. The clustering and specific adsorption may sterically hinder water adsorption to nearby sites until there is sufficient water to create a percolating network through the sample (Kulasinski et al. 2014). Moreover, RH values above 75 % or EMCs above 9 % have been linked to void or capillary filling (Kulasinski et al. 2014; Mazeau et al. 2015). Unlike cellulose fibrils in BC, pulp fibrils are further arranged into denser cell wall structures (Fig. 2d and insets in Fig. 3) (Castro et al. 2012; Dufresne 2012; Klemm et al. 1998, 2001), which give rise to more microporosity and therefore could partially cause the larger hysteresis at RH > 74 % observed for pulp. Both constricted and non-constricted pores can cause hysteresis via various effects, including the inkbottle effect and different menisci shapes during adsorption and desorption (Cohan 1938). However, surface area (i.e. porosity) had only a limited correlation to hysteresis (Fig. 6b).

The rates of adsorption and desorption were similar for the d-ND sample except for the first adsorption cycle. This might be due to the fact that the ND samples still have numerous open pores during the adsorption phase of the first cycle (Fig. 2d, Table 3) which allows the water a rapid access inside the fiber cell walls. Interestingly, the first cycle desorption rate is already very similar to that of the second cycle although EMC was much higher during the first half of desorption in the first cycle. During the desorption the water is present on the surfaces and inside amorphous cellulose, and specifically during the first cycle desorption, as liquid in microcapillaries. Although the total volume of the water is larger during the first cycle, it is not free to move in a similar manner to the water vapor during the first adsorption but is more like liquid or surface-bound water during the second desorption, hence the desorption kinetics are more alike. When water evaporates during the first desorption, it pulls the fibrils towards each other due to capillary pressure and closes the pores as it retracts. As a result, the RH value where the EMC's of the two cycles coincide might indicate the point where this structural collapse is complete. For d-ND it was ca 23 % RH (Fig. 2a) which coincides well with the lowest RH outlined in the literature for hornification by Weise *et al*. (1996), who reported that hornification occurs at 20-75 % solids content, depending on the pulp type.

Gradual hygroscopic changes

The DVS isotherms show gradual changes in hygroscopicity as RH is changed. In the d-ND-g isotherms it can be seen that part of the hygroscopic changes related to the RH maxima already occur by the time the previous cycle to lower RH maximum was completed. For example, as the adsorption data point of d-ND-g at 79 % RH is roughly halfway between that of cycles 1 and 2

559 of d-ND, the previous d-ND-g cycle up to 69 % RH had resulted in approximately half of the
560 changes, which would have been caused by one complete cycle to 93 % RH (Fig. 2b). This
561 shows that the sample had some area that remained relatively unaffected until a sufficiently high
562 RH was reached. Once a suitably high RH was achieved and the sample had been subsequently
563 dried, most of the potential changes due to that particular RH for the cellulose sample were
564 complete. Since cellulose swells and opens up as its EMC increases, the different RH values
565 could be related to different locations in the sample. Similar conclusions on cellulose and wood
566 (Greyson and Levi 1963; Taniguchi et al. 1978) have been reported to occur due to water
567 returning to the same sorption sites at repeated RH levels. Taniguchi *et al*. showed that
568 deuterium labeled hydroxyls in wood were not increased by repeating similar exposures but only
569 after exposing the samples to increasingly high D_2O humidities. Interestingly, they observed no
570 further changes with cycles extending above 60 % RH, which is not the case with DVS data
571 outlined here. On the other hand, Greyson and Levi reported incremental reductions in N_2 SSA
572 as water vapor exposure cycles were taken to incrementally higher RH's. With full DVS cycles it
573 is possible to study factors behind these phenomena more in detail.

574

575 At least two phases could be identified in the sample responses when they were exposed to water
576 vapor: first hydroxyl group accessibility was lowered at that RH (or "that sample location") as
577 water penetrated and retracted from it for the first time. After the sample was exposed to 10-20
578 % RH units higher conditions and water penetrated deeper in the sample, the hydroxyl
579 accessibility increased again at the earlier location (Fig. 2c). Interestingly, newly available
580 sorption sites do not only appear near the new maximum but at all RH values > 10-20 % RH
581 units below the new maximum. The experiment with repeated cycles at 59 and 69 % RH

supports these observations as, for example, sorption at < 40 % RH did not proceed during the repetitive cycles at 59 and 69 % RH nearly as much as when the exposure humidity was increased finally to 79 % RH. More sorption sites become accessible after a new peak RH is attained. Additionally, the results from K-ND-g suggest that hygroscopic changes are more reversible the closer the analyzed RH is to the previous RH maximum. Since the sorption stayed almost constant < 38 % RH while it was changing at 49-69 % RH during the repetitive cycles, it implies that the changes (hornification) are more irreversible in the RH values near the exposure maximum, or the corresponding sample location, after water has advanced and retracted from locations deeper within the sample.

Additionally, the kinetic data show an anomaly at 10-20 % RH units below each cycle maximum. With d-ND-g the highest RH measurement of a cycle took less time than the same RH measurement during the next one or two cycles (Fig. 6b), as if prior exposure to the exact same RH had made adsorption more difficult. This coincides well with the EMC minimum observed in the isotherms (Fig. 2c), which in combination with the longer step lengths (Fig. 6b) causes the adsorption rate to reach a local minimum at 10-20 % units below the previous RH maximum (not shown). Furthermore, also the kinetic effect was lost after the sample had been exposed to 20 % units higher RH and subsequently dried. Interestingly, the anomaly was not observed during desorption which indicates that the largest changes in water accessibility occur during adsorption.

On the SSA comparisons based on N_2 and H_2O adsorption

The comparison of H_2O and N_2 sorption data (Table 3) brings new arguments to the long-lasting issue on whether the two methods are comparable. Firstly, strong interactions between adsorbate molecules is not compatible with assumptions of monolayer coverages or BET theory (Sing 2014). Secondly, water has already been reported to be unsuitable for surface area determinations for even rather stiff samples (Robens et al. 2004) and cellulose could be expected to be worse as water can open up structures as it penetrates into soft and hygroscopic matter. Such penetration creates smaller fractal like porosity or surfaces (Liao et al. 2012; Stone and Scallan 1966; Strømme et al. 2003) which effectively means that there is no stable "surface" to be studied due to sample dynamism as RH is being changed. This is supported by observation that there were no expected changes in isotherm shape or adsorption heat at RH values where water monolayer should have been completed (Greyson and Levi 1963). Nevertheless, even recently researchers have been using water as a probe molecule in specific surface area analysis which has shown high surface areas in comparison to typical nitrogen adsorption data (Espino-Pérez et al. 2016; Häggkvist et al. 1998; Ioelovich and Leykin 2011; Klemm et al. 1998; Rowen and Blaine 1947; Zografi et al. 1984). Some of the authors have even used this as a proof for their conclusions on sample properties. Confusingly, there has also been attempts to correct nitrogen sorption values closer to water sorption values, which may have differed even by orders of magnitudes for some systems (Caurie 2012). In fact these differences might be caused by different sample drying methods as N_2 adsorption is generally more sensitive to cellulose aggregations than H_2O (Table 3). Especially for the most porous samples our results show occasionally larger SSA values for H_2O than N_2 adsorption. This brings even more seriously into question the validity of previously published arguments and conclusions on comparisons between the two methods.

Conclusions

Exposing wet cellulosic samples first to low-polar liquids and then to water vapor was shown to cause various hygroscopic changes. First hygroscopicity was reduced during the low-polar treatment, when the initial water was removed from the samples with acetone and supercritical CO_2. When the samples were subsequently exposed to water vapor, the fibrils aggregated and the hygroscopicity was further reduced near the exposure maximum. Nevertheless, sample hygroscopicity increased at Relative Humidity (RH) values more than 10-20 % RH units below the maximum. Additionally, the increase was partially reversible in ambient conditions near the exposure maximum. These changes were likely as a result of surface restructuring back to a more hygroscopic form as water gradually penetrated and retracted from new locations within the sample. Interestingly, hornification reduced the observed changes which suggests it can prevent surface restructuring and especially prevent hygroscopic loss during the low polar treatments. The procession of hygroscopic changes and hornification were observable with DVS, however, water adsorption isotherms were shown to be unable to measure cellulosic surface areas, therefore as a consequence the application of BET or similar methods to water isotherms is strongly discouraged in cellulose studies. Additionally, the exposure histories should be reported for cellulosic samples when adsorption studies are published.

ACKNOWLEDGMENTS

This work was a part of ACel program of the Finnish Bioeconomy Cluster FIBIC. The funding of the Finnish Funding Agency for Technology and Innovation (TEKES) and the Academy of Finland (POROFIBRE project) is acknowledged. Katarina Dimic-Misic is thanked for providing the BC. Benjamin Wilson is thanked for proofreading. Henna Penttinen is thanked for the initial literature review in her interesting undergraduate thesis on cellulose surfaces in environments with different polarities. This work made use of the Aalto University Nanomicroscopy Center (Aalto-NMC) premises.

Conflict of Interest

The authors declare that they have no conflict of interest.

REFERENCES

Atalla RH, Brady JW, Matthews JF, Ding S-Y and Himmel ME (2008) Structures of Plant Cell Wall Celluloses. In: Biomass Recalcitrance. Blackwell Publishing Ltd. Doi: 10.1002/9781444305418.ch6

Banik G, Brückle I (2010) Principles of water absorption and desorption in cellulosic materials. Restaurator 31:164–77. doi: 10.1515/rest.2010.012

Bazooyar F, Bohlén M, Bolton K (2015) Computational studies of water and carbon dioxide interactions with cellobiose. J Mol Model 21:16. doi: 10.1007/s00894-014-2553-5

Belbekhouche S, Bras J, Siqueira G, Chappey C, Lebrun L, Khelifi B, Marais S, Dufresne A. (2011) Water sorption behavior and gas barrier properties of cellulose whiskers and microfibrils films. Carbohydr Polym 83:1740–8. doi: 10.1016/j.carbpol.2010.10.036

Berthold J, Rinaudo M, Salmén L (1996) Association of water to polar groups; estimations by an adsorption model for ligno-cellulosic materials. Colloids Surfaces A 112:117–29. doi: 10.1016/0927-7757(95)03419-6

Bledzki AK, Gassan J (1999) Composites reinforced with cellulose based fibres. Prog Polym Sci 24:221–74. doi: 10.1016/S0079-6700(98)00018-5

675 Brunauer S, Emmett PH, Teller E (1938) Adsorption of gases in multimolecular layers. J Am
676 Chem Soc 60:309–19. doi: 10.1021/ja01269a023

677 Castro C, Zuluaga R, Álvarez C, Putaux JL, Caro G, Rojas OJ, Mondragon I, Gañán P (2012)
678 Bacterial cellulose produced by a new acid-resistant strain of Gluconacetobacter genus.
679 Carbohydr Polym 89:1033–7. doi: 10.1016/j.carbpol.2012.03.045

680 Caurie M (2012) A method to correct the wide discrepancy between Brunauer, Emmett and
681 Teller water and N2 surface areas of adsorbents. Int J Food Sci Tech 47:2366–71. doi:
682 10.1111/j.1365-2621.2012.03111.x

683 Chirkova J, Andersons B, Andersone I (2009) Study of the structure of wood-related
684 biopolymers by sorption methods. Bioresources 4:1044–57.

685 Christensen GN (1959) The rate of sorption of water vapor by wood and pulp. Appita J 13:112–
686 23.

687 Cohan LH (1938) Sorption hysteresis and the vapor pressure of concave surfaces. J Am Chem
688 Soc 60:433–5. doi: 10.1021/ja01269a058

689 Driemeier C, Mendes FM, Oliveira MM (2012) Dynamic vapor sorption and thermoporometry to
690 probe water in celluloses. Cellulose 19:1051–63. doi: 10.1007/s10570-012-9727-z

691 Dufresne A (2012) Cellulose and potential reinforcement. In: Nanocellulose - From nature to
692 high performance tailored materials. Walter de Gruyter GmbH, pp 1–42

693 Engelund ET, Thygesen LG, Svensson S, Hill CAS (2013) A critical discussion of the physics of
694 wood–water interactions. Wood Sci Technol 47:141–61. doi: 10.1007/s00226-012-0514-7

695 Espino-Pérez E, Bras J, Almeida G, Relkin P, Belgacem N, Plessis C, Domenek S (2016)
696 Cellulose nanocrystal surface functionalization for the controlled sorption of water and
697 organic vapours. Cellulose 23:2955–70. doi: 10.1007/s10570-016-0994-y

698 Fernandes AN, Thomas LH, Altaner CM, Callow P, Forsyth VT, Apperley DC, Kennedy CJ,
699 Jarvis MC (2011) Nanostructure of cellulose microfibrils in spruce wood. Proc Natl Acad
700 Sci USA 108:1195–203. doi: 10.1073/pnas.1108942108

701 Fernandes Diniz JMB, Gil MH, Castro JAAM (2004) Hornification — its origin and
702 interpretation in wood pulps. Wood Sci Technol 37:489–94. doi: 10.1007/s00226-003-
703 0216-2

704 Glass SV, Boardman CR, Zelinka SL (2017) Short hold times in dynamic vapor sorption
705 measurements mischaracterize the equilibrium moisture content of wood. Wood Sci
706 Technol 51:243–60. doi: 10.1007/s00226-016-0883-4

Grethlein HE (1985) The effect of pore size distribution on the rate of enzymatic hydrolysis of cellulosic substrates. Nat Biotechnol 3:155–60. doi: 10.1038/nbt0285-155

Greyson J, Levi AA (1963) Calorimetric measurements of the heat of sorption of water vapor on dry swollen cellulose. J Polym Sci Part A 1:3333–42. doi: 10.1002/pol.1963.100011106

Grunin LY, Grunin YB, Talantsev VI, Nikolskaya EA, Masas DS (2015) Features of the structural organization and sorption properties of cellulose. Polym Sci Ser A 57:43–51. doi: 10.1134/S0965545X15010034

Heiner AP, Kuutti L, Teleman O (1998) Comparison of the interface between water and four surfaces of native crystalline cellulose by molecular dynamics simulations. Carbohydr Res 306:205–20. doi: 10.1016/S0008-6215(97)10053-2

Hill CAS, Keating BA, Jalaludin Z, Mahrdt E (2012) A rheological description of the water vapour sorption kinetics behaviour of wood invoking a model using a canonical assembly of Kelvin-Voigt elements and a possible link with sorption hysteresis. Holzforschung 66:35–47. doi: 10.1515/HF.2011.115

Hill CAS, Norton A, Newman G (2009) The water vapor sorption behavior of natural fibers. J Appl Polym Sci 112:1524–37. doi: 10.1002/app.29725

Hubbe MA, Rojas OJ, Lucia LA, Sain M (2008) Cellulosic nanocomposites: a review. Bioresources 3:929–80.

Hult E, Larsson PT, Iversen T (2001) Cellulose fibril aggregation -- an inherent property of kraft pulps. Polymer (Guildf) 42:3309–14. doi: 10.1016/S0032-3861(00)00774-6

Häggkvist M, Li T-Q, Ödberg L (1998) Effects of drying and pressing on the pore structure in the cellulose fibre wall studied by 1H and 2H NMR relaxation. Cellulose 5:33–49. doi: 10.1023/A:1009212628778

Ioelovich M, Leykin A (2011) Study of sorption properties of cellulose and its derivatives. Bioresources 6:178–95.

Iwamoto S, Abe K, Yano H (2008) The effect of hemicelluloses on wood pulp nanofibrillation and nanofiber network characteristics. Biomacromolecules 9:1022–6. doi: 10.1021/bm701157n

Jalaludin Z (2011) The water vapour sorption behaviour of wood, Edinburgh Napier University

Johansson L-S, Tammelin T, Campbell JM, Setälä H, Österberg M (2011) Experimental evidence on medium driven cellulose surface adaptation demonstrated using nanofibrillated cellulose. Soft Matter 7:10917. doi: 10.1039/c1sm06073b

739 Khanjani P, Väisänen S, Lovikka V, Nieminen K, Maloney T, Vuorinen T (2017) Assessing the
740 reactivity of cellulose by oxidation with 4-acetamido-2,2,6,6-tetramethylpiperidine-1-oxo-
741 piperidinium cation under mild conditions. Carbohydr Polym 176:293–8. doi:
742 10.1016/j.carbpol.2017.08.092

743 Klemm D, Philipp B, Heinze T, Heinze U, Wagenknecht W (1998) General considerations on
744 structure and reactivity of cellulose. In: Comprehensive Cellulose Chemistry. Wiley-VCH
745 Verlag GmbH & Co. KGaA, pp 9–29

746 Klemm D, Schumann D, Udhardt U, Marsch S (2001) Bacterial synthesized cellulose - artificial
747 blood vessels for microsurgery. Prog Polym Sci 26:1561–603. doi: 10.1016/S0079-
748 6700(01)00021-1

749 Kohler R, Alex R, Brielmann R, Ausperger B (2006) A New Kinetic Model for Water Sorption
750 Isotherms of Cellulosic Materials. Macromol Symp 244:89–96. doi:
751 10.1002/masy.200651208

752 Kulasinski K, Derome D, Carmeliet J (2017) Impact of hydration on the micromechanical
753 properties of the polymer composite structure of wood investigated with atomistic
754 simulations. J Mech Phys Solids 103:221–35. doi: 10.1016/j.jmps.2017.03.016

755 Kulasinski K, Guyer R, Keten S, Derome D, Carmeliet J (2015) Impact of moisture adsorption
756 on structure and physical properties of amorphous biopolymers. Macromolecules 48:2793–
757 800. doi: 10.1021/acs.macromol.5b00248

758 Kulasinski K, Keten S, Churakov SV, Guyer R, Carmeliet J, Derome D (2014) Molecular
759 mechanism of moisture-induced transition in amorphous cellulose. ACS Macro Lett
760 3:1037–40. doi: 10.1021/mz500528m

761 Kymäläinen M, Havimo M, Louhelainen J (2014) Sorption properties of torrefied wood and
762 charcoal. Wood Mater Sci Eng 9:170–8. doi: 10.1080/17480272.2014.916348

763 Köhnke T, Gatenholm P (2007) The effect of controlled glucuronoxylan adsorption on drying-
764 induced strength loss of bleached softwood pulp. Nord Pulp Pap Res J 22:508–15. doi:
765 10.3183/NPPRJ-2007-22-04-p508-515

766 Lang ARG, Mason SG (1960) Tritium exchange between cellulose and water: accessibility
767 measurements and effects of cyclic drying. Can J Chem 38:373–87. doi: 10.1139/v60-053

768 Leppänen K, Andersson S, Torkkeli M, Knaapila M, Kotelnikova N, Serimaa R (2009) Structure
769 of cellulose and microcrystalline cellulose from various wood species, cotton and flax
770 studied by X-ray scattering. Cellulose 16:999–1015. doi: 10.1007/s10570-009-9298-9

771 Leuk P, Schneeberger M, Hirn U, Bauer W (2015) Heat of Sorption: A Comparison Between
772 Isotherm Models and Calorimeter Measurements of Wood Pulp. Dry Technol 34:563–73.
773 doi: 10.1080/07373937.2015.1062391

774 Liao R, Zhu M, Zhou Xin, Zhang F, Yan J, Zhu W, Gu C (2012) Molecular dynamics study of
775 the disruption of H-bonds by water molecules and its diffusion behavior in amorphous
776 cellulose. Mod Phys Lett B 26:1250088. doi: 10.1142/S0217984912500881

777 Lovikka VA, Khanjani P, Väisänen S, Vuorinen T, Maloney TC (2016) Porosity of wood pulp
778 fibers in the wet and highly open dry state. Microporous Mesoporous Mater 234:326–35.
779 doi: 10.1016/j.micromeso.2016.07.032

780 Matthews JF, Skopec CE, Mason PE, Zuccato P, Torget RW, Sugiyama J, Himmel ME, Brady
781 JW (2006) Computer simulation studies of microcrystalline cellulose Iβ. Carbohydr Res
782 341:138–52. doi: 10.1016/j.carres.2005.09.028

783 Maurer RJ, Sax AF, Ribitsch V (2013) Molecular simulation of surface reorganization and
784 wetting in crystalline cellulose I and II. Cellulose 20:25–42. doi: 10.1007/s10570-012-9835-
785 9

786 Mazeau K (2015) The hygroscopic power of amorphous cellulose: A modeling study. Carbohydr
787 Polym 117:585–91. doi: 10.1016/j.carbpol.2014.09.095

788 Medronho B, Duarte H, Alves L, Antunes F, Romano A, Lindman B (2015) Probing cellulose
789 amphiphilicity. Nord Pulp Pap Res J 30:58–66. doi: 10.3183/NPPRJ-2015-30-01-p058-066

790 Mihranyan A, Llagostera AP, Karmhag R, Strømme M, Ek R (2004) Moisture sorption by
791 cellulose powders of varying crystallinity. Int J Pharm 269:433–42. doi:
792 10.1016/j.ijpharm.2003.09.030

793 Mohan T, Spirk S, Kargl R, Doliška A, Vesel A, Salzmann I, Resel R, Ribitsch V, Stana-
794 Kleinschek K (2012) Exploring the rearrangement of amorphous cellulose model thin films
795 upon heat treatment. Soft Matter 8:9807–15. doi: 10.1039/c2sm25911g

796 Minor JL (1994) Hornification — its origin and meaning. Prog Pap Recycl 3:93–5.

797 Nelson R, Oliver DW (1971) Study of cellulose structure and its relation to reactivity. J Polym
798 Sci Pol Sym 36:305–20. doi: 10.1002/polc.5070360122

799 Newman RH (2004) Carbon-13 NMR evidence for cocrystallization of cellulose as a mechanism
800 for hornification of bleached kraft pulp. Cellulose 11:45–52. doi:
801 10.1023/B:CELL.0000014768.28924.0c

802 Newns AC (1973) Sorption and Desorption Kinetics of the Cellulose and Water System - Part 2.
803 J Chem Soc Faraday Trans 1 69:444–8. doi: 10.1039/F19736900444

804 Oksanen T, Buchert J, Viikari L (1997) The role of hemiocelluloses in the hornification of
805 bleached kraft pulps. Holzforschung 51:355–60. doi: 10.1515/hfsg.1997.51.4.355

806 Olsson A-M, Salmén L (2004) The association of water to cellulose and hemicellulose in paper
807 examined by FTIR spectroscopy. Carbohydr Res 339:813–8. doi:
808 10.1016/j.carres.2004.01.005

809 Pierce C, Wiley JW, Smith RN (1949) Capillarity and surface area of charcoal. J Phys Chem
810 53:669–83. doi: 10.1021/j150470a007

811 Robens E, Dąbrowski A, Kutarov VV (2004) Comments on surface structure analysis by water
812 and nitrogen adsorption. J Therm Anal Calorim 76:647–57. doi:
813 10.1023/B:JTAN.0000028044.44316.ce

814 Rowen JW, Blaine RL (1947) Sorption of nitrogen and water vapor on textile fibers. Ind Eng
815 Chem 39:1659–63. doi: 10.1021/ie50456a029

816 Salmén L (1982) Temperature and water induced softening behaviour of wood fiber based
817 materials, The Royal Institute of Technology, Stockholm

818 Sepall O, Mason SG (1961) Hydrogen exchange between cellulose and water: II. Interconversion
819 of accessible and inaccessible regions. Can J Chem 39:1944–55. doi: 10.1139/v61-261

820 Sing KSW (2014) Assessment of Surface Area by Gas Adsorption. In: Adsorption by Powders
821 and Porous Solids, 2nd edn. Elsevier Ltd., pp 237–68

822 Sing KSW, Everett DH, Haul RAW, Moscou L, Pierotti RA, Rouquérol J, Siemieniewska T
823 (1985) Reporting physisorption data for gas/solid systems with special reference to the
824 determination of surface area and porosity. Pure Appl Chem 57:603–19. doi:
825 10.1351/pac198557040603

826 Sinko R, Qin X, Keten S (2015) Interfacial mechanics of cellulose nanocrystals. MRS Bull
827 40:340–8. doi: 10.1557/mrs.2015.67

828 Siró I, Plackett D (2010) Microfibrillated cellulose and new nanocomposite materials: A review.
829 Cellulose 17:459–94. doi: 10.1007/s10570-010-9405-y

830 Stone JE, Scallan AM (1967) The effect of component removal upon the porous structure of the
831 cell wall of wood. II. Swelling in water and the fiber saturation point. Tappi J 50:496–501.

832 Stone JE, Scallan AM (1966) Influence of drying on the pore structures of the cell wall. In:
833 Consolidation of the paper web: Transactions of the symposium held at Cambridge. pp 145–
834 74

Strømme M, Mihranyan A, Ek R, Niklasson GA (2003) Fractal dimension of cellulose powders analyzed by multilayer BET adsorption of water and nitrogen. J Phys Chem B 107:14378–82. doi: 10.1021/jp034117w

Suchy M, Kontturi E, Vuorinen T (2010a) Impact of drying on wood ultrastructure: Similarities in cell wall alteration between native wood and isolated wood-based fibers. Biomacromolecules 11:2161–8. doi: 10.1021/bm100547n

Suchy M, Virtanen J, Kontturi E, Vuorinen T (2010b) Impact of drying on wood ultrastructure observed by deuterium exchange and photoacoustic FT-IR spectroscopy. Biomacromolecules 11:515–20. doi: 10.1021/bm901268j

Taniguchi T, Harada H, Nakato K (1978) Determination of water adsorption sites in wood by a hydrogen–deuterium exchange. Nature 272:230–1. doi: 10.1038/272230a0

Thybring EE, Thygesen LG, Burgert I (2017) Hydroxyl accessibility in wood cell walls as affected by drying and re-wetting procedures. Cellulose 24:2375–84. doi: 10.1007/s10570-017-1278-x

Timmermann EO (2003) Multilayer sorption parameters: BET or GAB values? Colloids Surfaces A 220:235–60. doi: 10.1016/S0927-7757(03)00059-1

Topgaard D, Söderman O (2001) Diffusion of Water Absorbed in Cellulose Fibers Studied with 1 H-NMR. Langmuir 17:2694–702. doi: 10.1021/la000982l

Weatherwax RC (1977) Collapse of cell-wall pores during drying of cellulose. J Colloid Interf Sci 62:432–46. doi: 10.1016/0021-9797(77)90094-7

Weatherwax RC, Caulfield DF (1971) Cellulose aerogels: an improved method for preparing a highly expanded form of dry cellulose. Tappi J 54:985–6.

Weise U, Maloney T, Paulapuro H (1996) Quantification of water in different states of interaction with wood pulp fibres. Cellulose 3:189–202. doi: 10.1007/BF02228801

Willems W (2014a) The water vapor sorption mechanism and its hysteresis in wood: the water/void mixture postulate. Wood Sci Technol 48:499–18. doi: 10.1007/s00226-014-0617-4

Willems W (2014b) Hydrostatic pressure and temperature dependence of wood moisture sorption isotherms. Wood Sci Technol 48:483–98. doi: 10.1007/s00226-014-0616-5

Xie Y, Hill CAS, Jalaludin Z, Curling SF, Anandjiwala RD, Norton AJ, Newman G (2010) The dynamic water vapour sorption behaviour of natural fibres and kinetic analysis using the parallel exponential kinetics model. J Mater Sci 46:479–89. doi: 10.1007/s10853-010-4935-0

868 Xie Y, Hill CAS, Jalaludin Z, Sun D (2011) The water vapour sorption behaviour of three
869 celluloses: analysis using parallel exponential kinetics and interpretation using the Kelvin-
870 Voigt viscoelastic model. Cellulose 18:517–30. doi: 10.1007/s10570-011-9512-4

871 Yamane C, Aoyagi T, Ago M, Sato K, Okajima K, Takahashi T (2006) Two different surface
872 properties of regenerated cellulose due to structural anisotropy. Polym J 38:819–26. doi:
873 10.1295/polymj.PJ2005187

874 Zheng Y, Lin H, Tsao GT (1998) Pretreatment for cellulose hydrolysis by carbon dioxide
875 explosion. Biotechnol Prog 14:890–6. doi: 10.1021/bp980087g

876 Zografi G, Kontny MJ, Yang AYS, Brenner GS (1984) Surface area and water vapor sorption of
877 microcrystalline cellulose. Int J Pharm 18:99–116. doi: 10.1016/0378-5173(84)90111-X

878 Zografi G, Kontny MJ (1986) The interactions of water with cellulose- and starch-derived
879 pharmaceutical excipients. Pharm Res 3:187–94. doi: 10.1023/A:1016330528260

880